

# Indirect consequences of exciplex states on the phosphorescence lifetime of phenazine-based 1,2,3-triazole luminescent probes

Bárbara B. A. Costa<sup>1</sup>, Guilherme A. M. Jardim<sup>2</sup>, Paloma L. Santos<sup>3</sup>, Hállen D. R. Calado<sup>2</sup>, Andrew P. Monkman<sup>3</sup>, Fernando B. Dias<sup>3</sup>, Eufânio N. da Silva Júnior<sup>2</sup>, Luiz A. Cury<sup>1†</sup>

<sup>1</sup>*Instituto de Ciências Exatas, Departamento de Física,*

*Universidade Federal de Minas Gerais, 31270-901, Belo Horizonte, Minas Gerais, Brazil*

<sup>2</sup>*Instituto de Ciências Exatas, Departamento de Química,*

*Universidade Federal de Minas Gerais, 31270-901, Belo Horizonte, Minas Gerais, Brazil*

<sup>3</sup>*Department of Physics, University of Durham, South Road DH1 3LE, Durham, United Kingdom*

(Dated: August 12, 2016)

The optical properties of phenazine derivative probe solutions involving intersystem crossing from singlet to triplet states were investigated by time resolved spectroscopy. The room temperature phosphorescent emission presented different time responses when  $Cd^{2+}$  ions were bound to the probe chemical structure. The complex exciplex formation observed to occur in this case was not directly responsible for the change in the phosphorescence lifetime. This was more influenced by the new molecular conformation and modified spin-orbit coupling imposed by the binding of the  $Cd^{2+}$  ions to the phenazine molecules.

## I. INTRODUCTION

Simple phenazine (PZ) backbone structure possess a relatively weak fluorescence quantum yield due to the predominant singlet decay via intersystem crossing (ISC).<sup>1-5</sup> Despite their lack of fluorescence emission, phenazine molecules could be useful in Biological systems. Related studies indicated that they would interact directly with biocompounds such DNA bases via photoinduced electron transfer.<sup>6</sup> On the other hand, PZ derivatives can present appreciable fluorescence<sup>7-10</sup> enabling their specific use as fluorescent probes in biological environment, where small quantities are enough to be detected without disturbing the system in study. Some PZ derivatives can also present steady-state phosphorescence, relatively weak but observable at room temperature.<sup>11</sup> The detection of phosphorescence properties of PZ or PZ derivatives through gated intensified charge-coupled devices (iCCD's), would be also useful as a second experimental signature in order to use them as markers in intra-cellular or related media. In an early work,<sup>12</sup> a PZ derivative was designed and synthesized, being used lately as selective metal sensor and demonstrating selectivity for cadmium ions, which are very dangerous for the human life. The cadmium ions selectivity was identified via fluorescence enhancement due to exciplex formation. The formation of singlet exciplex complex have been reported in the recent past in blended PZ with *N,N*-diethylaniline, *N,N*-dimethylaniline and 4,4'-bis(dimethylamino)diphenylmethane.<sup>13,14</sup> The occurrence of singlet complex exciplex in PZ based systems would mean the presence of a concurrent channel that would consume the singlet PZ states for the formation of the exciplex states, avoiding part of them to decay

via ISC to PZ triplet states. In this work, the exciplex formation occurs due to the interaction of cadmium ions with the PZ derivative structure. The exciplex dominates the singlet emission but ISC mechanism in the PZ derivative to the triplet manifold is still allowed. Thus, by means of time resolved fluorescence measurements we had the access to phosphorescent properties as well as delayed emissions via reverse ISC in our phenazine derivative. The consequences of the complex exciplex formation on the optical transitions coming from the PZ derivative triplet states were discussed, enlarging the overall knowledge of phenazine structures as potential phosphorescent materials not only for biological but also electro-optical applications.

## II. SAMPLES AND EXPERIMENTAL DETAILS

The synthesis of the phenazine-based 1,2,3-triazole luminescent probe made from the available natural product lapachol, extracted from the heartwood of *Tabebuia sp.* (Tecoma), was successfully accomplished. The synthetic route and the details of the photophysics properties of the final phenazine-based *N,N*-bis(2-picoly1)-amine probe and its potentiality for  $Cd^{2+}$  selectivity at the micromolar level was reported in our early work.<sup>12</sup> The formation of a complex exciplex emission was observed on the fluorescence spectrum of the probe+ $Cd^{2+}$  in comparison to that of the probe solution. The exciplex formation was characterized and confirmed by the nonexistence of any spectral feature on the absorption spectrum and by time correlated single photon counting (TCSPC) measurements. In order to explore the consequences of the exciplex formation on the singlet-triplet direct and reverse intersystem crossing on these phenazine derivative systems the probe and the probe+ $Cd^{2+}$  solutions were analyzed by means of delayed fluorescence measurements.

The standard photoluminescence (steady-state) and photoluminescence excitation measurements were per-

<sup>†</sup>Corresponding author. E-mail address: cury@fisica.ufmg.br

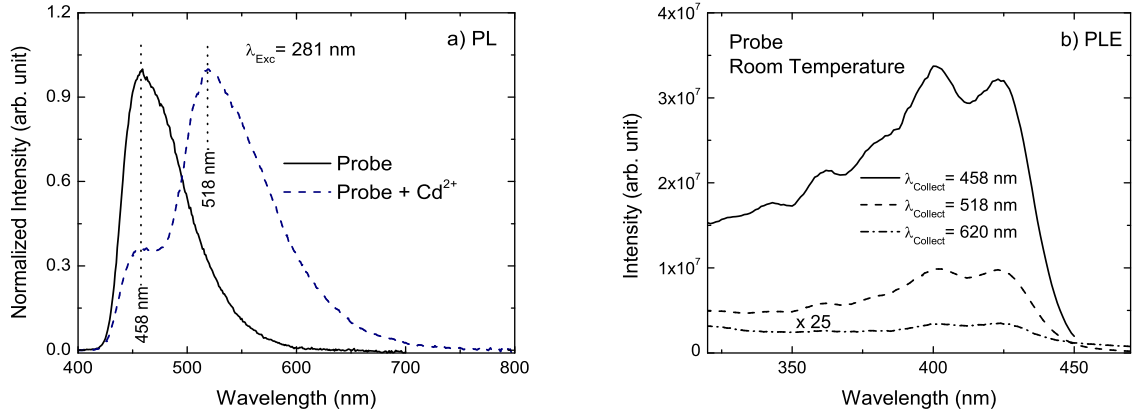


FIG. 1: (Color online) (a) Steady-state Photoluminescence emission for the probe and the probe+ $Cd^{2+}$  solutions at room temperature with the excitation made at  $\lambda_{Exc} = 281 \text{ nm}$ . Photoluminescence excitation spectra (PLE) at room temperature for the probe (b) solution collected at  $\lambda_{Collect} = 458 \text{ nm}$ ,  $518 \text{ nm}$  and  $620 \text{ nm}$ . The PLE spectra collected at  $\lambda_{Collect} = 458 \text{ nm}$  and  $518 \text{ nm}$  correspond to the peak of the probe emission and to the exciplex peak emission of the probe+ $Cd^{2+}$ , respectively. The PLE spectra collected at  $\lambda_{Collect} = 620 \text{ nm}$  (x25), as will be discussed in the text, is correlated to the phosphorescence emission of our phenazine derivative.

formed in a Jobin Yvon Horiba Fluorolog fluorimeter at room temperature and in the air. Time-resolved photoluminescence decays were collected using the picosecond time correlated single photon counting (TC-SPC) technique (instrument response function  $24 \text{ ps}$ ,  $76 \text{ MHz}$  repetition rate). The solutions were excited by a third harmonic pulse ( $\lambda = 281 \text{ nm}$ ) from a mode-locked Ti:sapphire laser from Coherent Inc., with vertical polarization. The emission was detected through a double-subtractive monochromator (SpectraPro-2300i), and a MCP detector (Hamamatsu model R3809U-50) was used to collect decays at  $454 \text{ nm}$ ,  $519 \text{ nm}$  and at  $620 \text{ nm}$ .

Phosphorescence, prompt fluorescence (PF), and delayed fluorescence (DF) spectra and decays were recorded using nanosecond gated luminescence and lifetime measurements (from  $40 \text{ ns}$  to  $5 \mu\text{s}$ ) using a high energy pulsed Nd:YAG laser emitting at  $355 \text{ nm}$  (EKSPLA). Both probe and the probe+ $Cd^{2+}$  solutions studied here show relatively strong delayed fluorescence and phosphorescence at room temperature in a degassed mixture of water:acetonitrile ( $8.5 : 1.5$ ). The probe+ $Cd^{2+}$  solution was produced using 1 per 1 equivalent of the probe molecule per  $Cd^{2+}$  ions. A solution of the probe in ethanol ( $0.05 \text{ mg/mL}$ ) was also studied in order to confirm its phosphorescence properties at lower temperatures. Emissions were focused onto a spectrograph and detected on a sensitive gated iCCD camera (Stanford Computer Optics) having sub-nanosecond resolution. Phosphorescence, PF and DF time resolved measurements were performed by increasing gate and delay times.

### III. RESULTS AND DISCUSSIONS

The probe and the probe+ $Cd^{2+}$  solutions were firstly characterized by photoluminescence (PL) at room temperature. The respective PL spectra are shown in **Figure 1a**. The maximum PL emission for the probe occurs at  $458 \text{ nm}$  while for the probe+ $Cd^{2+}$  the formation of the exciplex complex redshifts the maximum emission to  $518 \text{ nm}$ . Exciplexes are entities that only exist at excited states, thus the basic absorption characterization of the probe and the probe+ $Cd^{2+}$  solutions was made just to confirm that any new features in the absorption spectra would be observed. The absorption spectra for the probe and the probe+ $Cd^{2+}$  solutions are shown in **Figure 1** of the support information (SI). In the place of absorption we show in **Figures 1b** very similar photoluminescence excitation (PLE) spectra taken for the probe solution at the collect positions of  $\lambda_{Collect} = 458$ ,  $518$  and  $620 \text{ nm}$ .

In order to investigate the intersystem crossing (ISC) effects and the optical properties coming from the triplet manifold in our probe and probe+ $Cd^{2+}$  we have performed time resolved fluorescence measurements. Measurements using time correlated single photon counting (TCSPC) technique were also made for complementary discussion. The probe and probe+ $Cd^{2+}$  solutions were previously degassed by purging pure  $N_2$  gas during about  $20 \text{ min}$  prior to the optical measurements.

In **Figure 2a** the Log-Log graphic displays the integrated intensity of the probe emission spectra for the prompt fluorescence (PF), with delay times at time scale of nanoseconds ( $ns$ ), and for the delayed fluorescence (DF), with delay times at time scale of microseconds ( $\mu\text{s}$ ). The PF and DF behaviors as a function of the de-

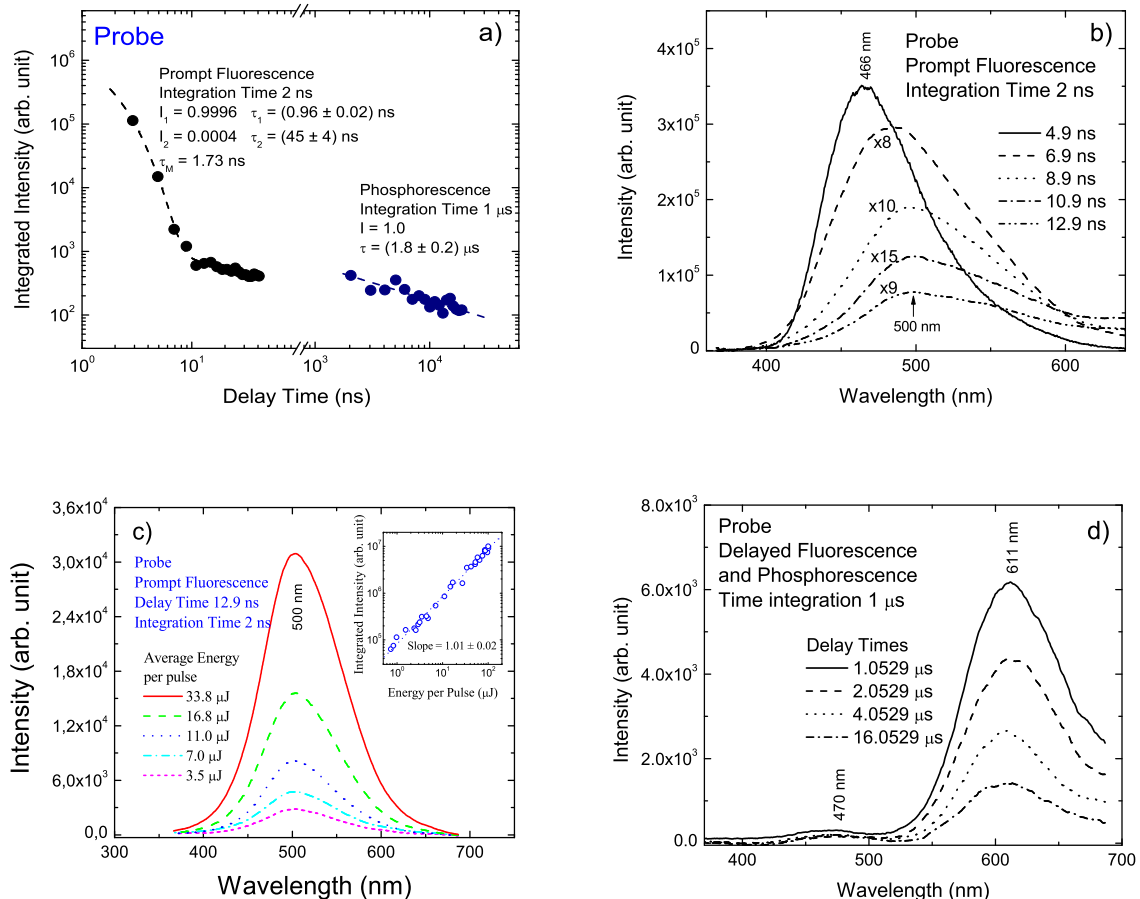


FIG. 2: (Color online) (a) Integrated intensity of the emission spectra for the prompt fluorescence (PF) and delayed fluorescence (DF) for the probe at room temperature as a function of delay time. The integration time used to collect the PF spectra was 2 ns while for the DF spectra we have used 1  $\mu$ s. The fitting curves (dashed lines) and corresponding lifetimes and the respective intensities are included in the figure.  $\tau_M$  is the average lifetime of the PF emission. (b) PF representative spectra at different delay times. The spectra were multiplied by respective factors for sake of visibility. (c) PF representative spectra for different average laser energy taken at a delay time of 12.9 ns. The inset shows the linear behavior of the integrated intensity with increasing the average laser energy. (d) DF representative spectra at different delay times. Note the time scale of  $\mu$ s. The faint band centered at around 470 nm comes from triplet to singlet states via reverse ISC and as expected it has the same shape of PF spectra. The more intense band, centered at 611 nm, is assigned to phosphorescent emission.

lay time were fitted respectively by a biexponential and monoexponential decays (dashed lines). The values of lifetimes and respective intensities are shown inside the figure. In **Figure 2b** the PF representative spectra, with the respective multiplication factors are shown as a function of different delay times. The PF spectra show a significant red-shift with increasing delay time. This excited state relaxation is probably due to local interactions between the probe excited state and solvent molecules. With increasing the average laser power (**Figure 2c**) the integrated intensity of the PF spectra increases linearly as shown in the inset of the figure. The delayed fluorescence (DF) spectra occurring in a  $\mu$ s time scale are shown in **Figure 2d**. Those spectra were obtained exciting the probe solution at a relatively weak average laser power

of 13  $\mu$ J per pulse. At that level of excitation we observe faint emissions for the band around 470 nm. This band is assigned as delayed fluorescence of the probe coming from triplet to singlet states via reverse ISC processes. As expected this band has the same PF shape because the final recombination comes from the same PF singlet states. This becomes clear at higher average laser power as shown in **Figure 3a** where the relative intensity of the band around 470 nm is much higher.

The band around 610 nm in **Figures 2d** and **3a** is assigned to the phosphorescent emission. There is no equivalence of such a band in the probe PF emission (**Figure 2b**). The integrated intensity of the bands at 464 nm and 608 nm as a function of the average laser energy are shown in **Figure 3b**. In **Figures 3a** and **3b**

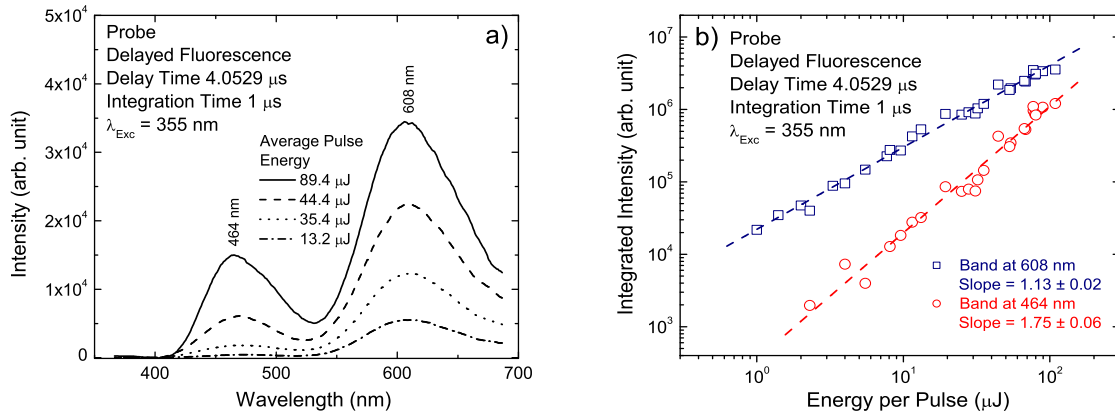


FIG. 3: (Color online) (a) DF representative spectra for the probe solution collected at 4.0529  $\mu\text{s}$  of delay time for different average laser energies. The band shape of delayed fluorescence at 464 nm coming from reverse ISC has the same shape as the PF spectra seem in **Figure 2b**. The band at 608 nm corresponds to the phosphorescent emission. (b) The integrated intensities of the bands at 464 nm and 608 nm as a function of the average laser energy. The respective growing rates are indicated in the figure.

we are dealing with degassed probe solution where the only triplet states are those populated via ISC singlet transfer. The slope of  $(1.75 \pm 0.06)$  corresponding to the band at 464 nm approaches the value of 2, which strongly suggests TTA mechanism at a regime of relatively low laser intensities.<sup>17</sup> For the band at 608 nm the growing rate  $(1.13 \pm 0.02)$  reconfirms what was expected for phosphorescent recombination.

Measurements made at room temperature, without degassing a probe solution in ethanol, put in evidence the phosphorescent nature of the band around 610 nm. The phosphorescence intensity vanishes due to presence of oxygen atoms immersed in the solution. Oxygen atoms in their fundamental states represent an excess of triplet states see **Figure 4a**. Thus, triplet-triplet annihilation (TTA) processes<sup>15,16</sup> occur in disadvantage to the radiative phosphorescent process. In addition, for the degassed solution in ethanol, the phosphorescent emission intensity (around 600 nm) clearly increases with decreasing temperature (**Figure 4b**). A slow decay of the phosphorescent emission at 80 K is observed (**Figure 4c**) and a relatively long lifetime of  $(625 \pm 80)$  ms was measured (**Figure 4d**), as expected.

The Log-Log graphic for the integrated intensity of the prompt (PF) and delayed (DF) fluorescence spectra for the probe+ $Cd^{2+}$  as a function of delay time is shown in **Figure 5a**. The dashed lines are the fitting curves, both representing biexponential decays. The corresponding lifetimes and respective intensities are shown inside the figure. The longer time component [ $\tau_2 = (9 \pm 1)$  ns] is assigned to the exciplex emission. The shorter time component [ $\tau_1 = (3.59 \pm 0.03)$  ns] of the probe becomes only important for the earlier times of the decay curve. The PF spectra (**Figure 5b**) are dominated by the ex-

ciplex emission (centered at 523 nm). This corresponds to the same characteristics observed in the steady-state PL spectrum shown in **Figure 1a**. The only signature of the original probe emission in **Figure 5b** is given by the shoulder around 450 nm that practically vanishes for delay times longer than 4 ns. For the DF emission of probe+ $Cd^{2+}$  (**Figure 5c**) the dominant phosphorescent band centered around 610 nm is relatively more intense in scale than in the case of probe solution at the same experimental conditions (**Figure 2d**). The intensities of the bands around 470 nm appear very faint even at higher average laser powers (**Figure 5d**). The relative decrease of the band intensity at 470 nm in relation to the phosphorescent band around 610 nm for the probe+ $Cd^{2+}$  is better seen by comparing **Figures 5d** and **3a**.

It is worth noticing that exciplex formation represents a new channel that would consume in part the donor singlet states of the probe solution. Thus, the greater the formation of exciplex states less will be the conversion of available singlet probe states into triplet states. This assumption would explain the relative decrease of the DF band intensity at 470 nm for the probe+ $Cd^{2+}$  observed in **Figures 5d**. Indeed, this was verified after investigating a probe+ $Cd^{2+}$  solution in excess of  $Cd^{2+}$  ions. No DF or phosphorescence emissions at all were observed for a probe+ $Cd^{2+}$  solution with a concentration corresponding to 1 per 2.5 equivalents of probe molecule to  $Cd^{2+}$  ions. In this case, only the PF appeared with the dominance of the exciplex peak emission. (See **Figure 2** and related discussion in the support information (SI).)

In our probe molecule, despite the lack of a heavy atom on it, the spin-orbit interaction would most likely occur due to increased excited state ISC induced by the nitrogen lone-electron pair on the main phenazine back-

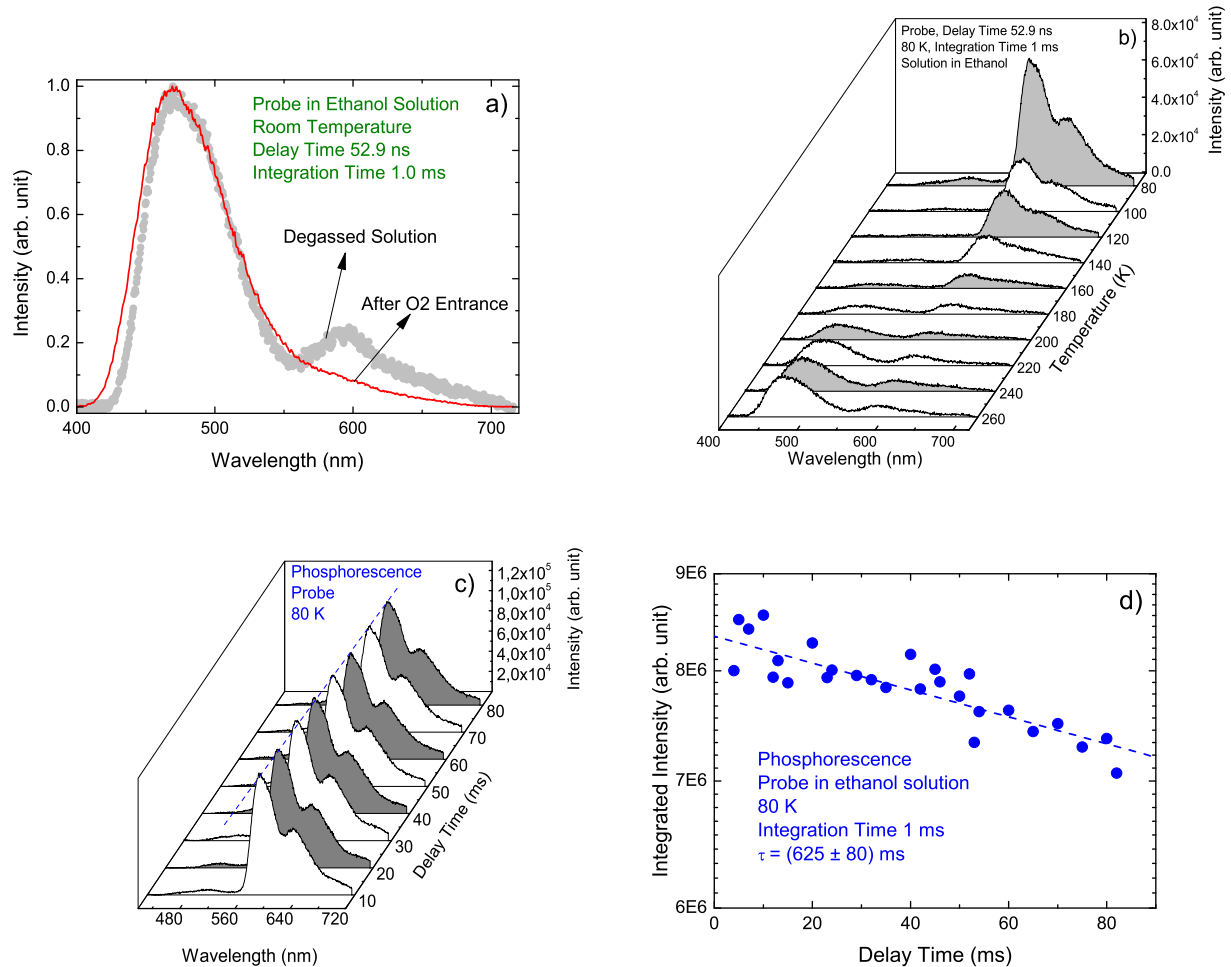


FIG. 4: (Color online) (a) Probe delayed fluorescence and phosphorescence peaks of the derivative phenazine solution in ethanol with and without degassing, taken at a delay time of 52.9 ns. (b) Increase of the phosphorescent emission intensity (around 600 nm) with decreasing temperature. (c) Phosphorescent emission spectra at different delay times illustrating the relatively slow intensity decay. (d) The monoexponential decay curve of the phosphorescence emission and the corresponding lifetime of  $(625 \pm 80) \text{ ms}$ .

bone structure.<sup>11</sup> Once the binding of  $Cd^{2+}$  ions is occurring just at these nitrogen sites<sup>12</sup> (see **Figure 3** in the **SI**) we can infer that the corresponding modified spin-orbit coupling takes place in there for the probe+ $Cd^{2+}$  molecules. The binding of the  $Cd^{2+}$  ions also induces a new molecular conformation to the probe molecule. These combined effects are assigned to be responsible for the smaller lifetime (**Figure 6**) observed in the phosphorescent decay of the probe+ $Cd^{2+}$  solution.

The exciplex formation itself would not be connected to the faster ISC processes of the probe+ $Cd^{2+}$  solution. It occurs exclusively on the domain of the singlet states. The preponderance of exciplex emission on the prompt fluorescence (PF) spectra simply reduces the number

of probe states that would undergo ISC, causing the faint DF intensity of the band around 470 nm (**Figures 5c** and **5d**).

Looking at the transition region (**Figure 7**), corresponding to the time scale of the end of the prompt fluorescence (PF) to the beginning of delayed fluorescence (DF) (and also phosphorescence) for the probe+ $Cd^{2+}$ , we can clearly see that at delay times higher than 82.9 ns the exciplex emission (around 510 nm) vanishes and the phosphorescent peak at 620 nm shows up definitely after 222.9 ns. In another words, at the time scale of the phosphorescent emission (delay times of the order of  $\mu\text{s}$ ) the exciplex does not exist anymore. The molecular conformation of the probe+ $Cd^{2+}$ , on the other hand, would remain the same, in-

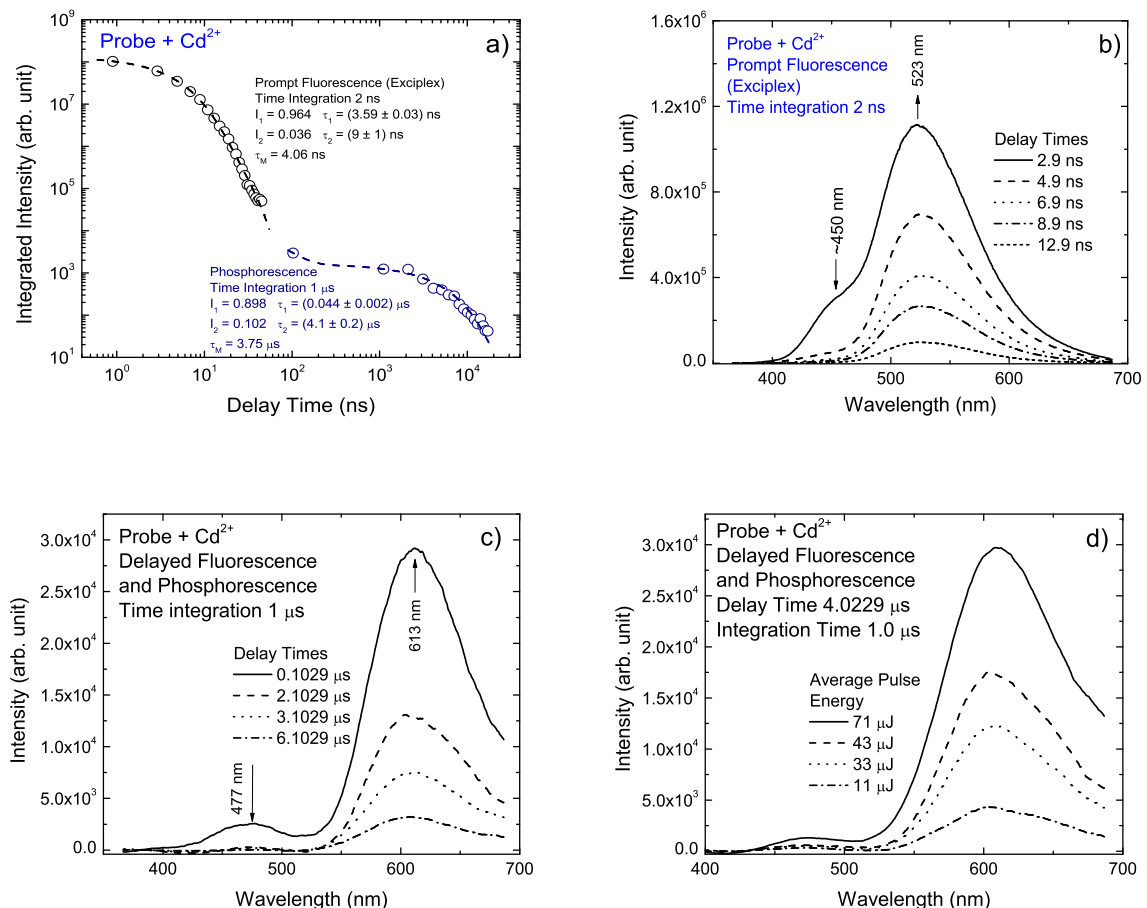


FIG. 5: (Color online) (a) Prompt fluorescence (PF) and delayed fluorescence (DF) for the probe+ $Cd^{2+}$  solution (1 Eq. : 1 Eq.) at room temperature as a function of delay time. The integration time used to collect the PF spectra was 2 ns while for the DF spectra we have used 1  $\mu$ s. The fitting curves (dashed lines) and corresponding lifetimes and the respective intensities are included in the figure.  $\tau_M$  is the average lifetime for the PF and DF emissions. (b) PF representative spectra at different delay times. The exciplex peak centered at 523 nm dominates the emission. (c) DF representative spectra for different delay times. A weak band around 470 nm appears but the phosphorescent band at 611 nm dominates the DF emission, even at higher average laser energies as shown in part (d).

variant on time, corroborating our interpretation of the faster ISC processes that occurs in this case due to a more effective spin-orbit coupling.

It is worth noticing that the conformational change of the probe molecule due to the binding of the  $Cd^{2+}$  ions did not have any consequence on the phosphorescent energy level. The phosphorescent band for the probe and probe+ $Cd^{2+}$  solutions appears practically at the same wavelength position.

TCSPC measurements for the probe and probe+ $Cd^{2+}$  were also performed to investigate the phosphorescent emission. The decay curves are shown in Figures 8a and 8b, respectively. They were collected at 454 nm, 519 nm and 620 nm, corresponding to the emission positions of

the probe, the exciplex, and the phosphorescent bands.

The steady-state PL spectra (Figure 1a) for the probe and probe+ $Cd^{2+}$  do not present any evidence of the phosphorescent emission at 620 nm. For the probe solution, with the main emission occurring around 460 nm, we would expect to obtain decay curves corresponding to average lifetimes that would not vary so much changing the wavelength around the peak position. That was the case for the wavelengths at 454 nm and 519 nm (see the average  $\tau_M$  values inside the figure). For the probe+ $Cd^{2+}$  solution (Figure 8b), the average lifetime of the decay at 454 nm was also very close to that obtained for the probe solution. At 519 nm, the relatively longer average lifetime

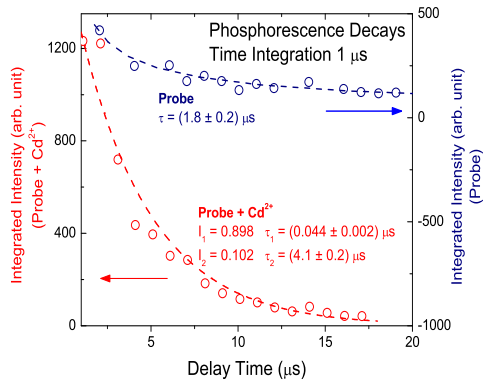


FIG. 6: (Color online) Phosphorescence decay curves for the probe+ $Cd^{2+}$  (left side) and probe (right side) solutions. The probe+ $Cd^{2+}$  decay is fitted by a biexponential curve, indicating a more complex molecular conformation due to the chemical complexation of  $Cd^{2+}$  ions with the derivative phenazine molecules, while the probe decay is fitted by just a monoexponential. Another great difference between them is the phosphorescence lifetime which is faster for the probe+ $Cd^{2+}$ , indicating a more effective spin-orbit interaction, and, therefore, faster ISC processes.

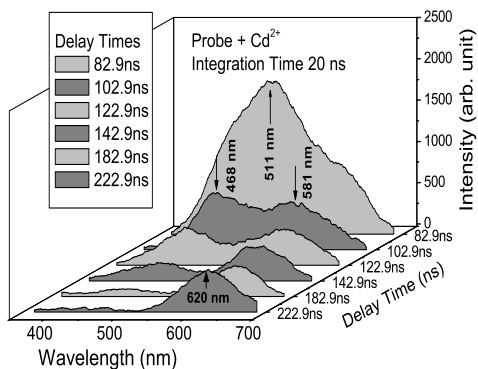


FIG. 7: Sequence of emission spectra for the probe+ $Cd^{2+}$  at delay times ranging from the end of the prompt fluorescence (PF) to the beginning of the delayed fluorescence (DF) (and also phosphorescence). Each one of the spectra were acquired with an integration time of 20 ns. For delay times higher than 82.9 ns the exciplex peak around 510 nm vanishes and the phosphorescence emission peak at 620 nm turns up.

was expected since it corresponded to the exciplex state in the probe+ $Cd^{2+}$  solution. However, at 620 nm, the decays for the probe and probe+ $Cd^{2+}$  presented unexpected longest lifetimes (Figures 8a and 8b) that could only be explained if correlated to the phosphorescent emission. Even though these TCSPC measurements do not represent definitive results they can be

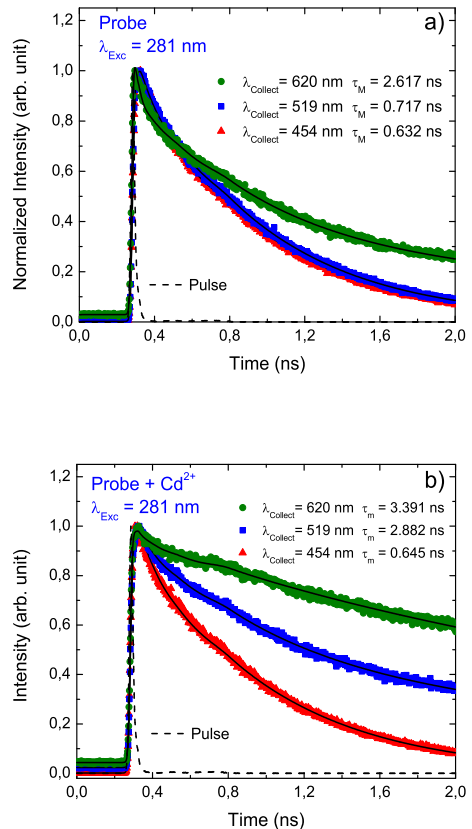


FIG. 8: (Color online) Room temperature time decay curves for the probe (a) and for the probe+ $Cd^{2+}$  (b) solutions with the excitation made at  $\lambda_{Exc} = 281$  nm and collected at  $\lambda_{Collect} = 454$  nm, 519 nm and 620 nm. The average values ( $\tau_M$ ) of the corresponding lifetimes are specified inside each figure. The dashed curves in parts (a) and (b) represent the time response of the TCSPC system. The full lines are the fits of the decay curves.

assigned as another indication of phosphorescent emission taking place at room temperature in our derivative phenazine solutions.

#### IV. CONCLUSIONS

In summary, the optical properties of triplet states in derivative phenazine solutions were investigated by time resolved spectroscopy at room temperature. The results for the probe solution show that singlet states undergo relatively high ISC to the triplet manifold, resulting in a back delayed fluorescence via TTA mechanism, which competes to the equally detected room temperature phosphorescent emission. For the probe+ $Cd^{2+}$  solution, the binding of the  $Cd^{2+}$  ions beyond inducing a new molecular conformation,

would modify the spin-orbit coupling of the lone-pair of nitrogen atoms in the phenazine backbone turning ISC processes faster and, consequently, more effective in order to reduce the lifetime of the probe+ $Cd^{2+}$  phosphorescent emission. The formation of exciplex states, in turn, reduces the density of probe singlet states. They would be completely extinguished at the time scale of the phosphorescent emission, which, therefore, would not have direct consequences on the probe+ $Cd^{2+}$  phosphorescence lifetime. On the other hand, the relatively decrease of the singlet ISC rate to triplet manifold causes a new time decay dynamics for the phosphorescence, and explains the relatively faint emission of delayed fluorescence band around 470 nm for the probe+ $Cd^{2+}$  solution.

## Acknowledgments

B. B. A. Costa, L. A. Cury, G. A. M. Jardim, H. D. R. Calado, E. N. da Silva Júnior thank FAPEMIG, CAPES, CNPq, the Instituto Nacional de Ciência e Tecnologia em Dispositivos Semicondutores (INCT-DISSE) from Brazil for the financial support. P. L. Santos thanks CAPES - Science Without Borders, for the Doctorate studentship, Proc. 12027/13-8. L. A. Cury and F. B. Dias also thank CAPES - Science Without Borders, for the PVE Program, Proc. 88881.030369/2013-01.

- 
- <sup>1</sup> Y. Hirata, I. Tanaka, *Chem. Phys. Lett.* 43(3) (1976) 568.
- <sup>2</sup> A. Grabowska, *Chem. Phys. Lett.* 1 (1967) 113.
- <sup>3</sup> T. G. Pavlopoulos, *Spectrochim. Acta* 43A (1987) 715.
- <sup>4</sup> J. I. DelBarrio, J. R. Rebato, F. M. G. Tablas, *J. Phys. Chem.* 93 (1989) 6836.
- <sup>5</sup> V. A. Kuz'min, P. P. Levin, *Bull. Acad. Sci. USSR Div. Chem. Sci.* 37 (1988) 1098.
- <sup>6</sup> S. D. Choudhury, S. Basu, *Spectrochim. Acta Part A* 62 (2005) 736.
- <sup>7</sup> M. K. Singh, H. Pal, A. C. Bhasikuttan, A. V. Sapre, *Photochem. Photobiol.* 68 (1998) 32.
- <sup>8</sup> C. E. M. Carvalho, I. M. Brinn, A. V. Pinto, M. C. F. R. Pinto, *J. of Photochem. Photobiol. A Chem: Part 3* 136 (2000) 25.
- <sup>9</sup> G. Gaertner, A. Grey, F. G. Holliman, *Tetrahedron* 18 (1962) 1105.
- <sup>10</sup> A. Grey, F. G. Holliman, *Tetrahedron* 18 (1962) 1095.
- <sup>11</sup> D. Chaudhuri, D. Li, E. Sigmund, H. Wettach, S. Höger, *J. M. Lupton, Chem. Commun.* 48 (2012) 6675.
- <sup>12</sup> G. A. M. Jardim, H. D. R. Calado, L. A. Cury, E. N. da Silva Júnior, *Eur. J. Org. Chem.* 2015(4) (2015), 703.
- <sup>13</sup> S. D. Choudhury, S. Basu, *Chem. Phys. Lett.* 373 (2003) 67.
- <sup>14</sup> S. D. Choudhury, S. Basu, *Chem. Phys. Lett.* 383 (2004) 533.
- <sup>15</sup> D. Y. Kondakov, T. D. Pawlik, T. K. Hatwar, J. P. Spindler, *J. Appl. Phys.* 106 (2009) 124510.
- <sup>16</sup> S. M. King, M. Cass, M. Pintani, C. Coward, F. B. Dias, A. P. Monkman, M. Roberts, *J. Appl. Phys.* 109 (2011) 074502.
- <sup>17</sup> V. Jankus, E. W. Snedden, D. W. Bright, V. L. Whittle, J. A. G. Williams, A. P. Monkman, *Adv. Funct. Mater.* 23 (2013) 384.
- <sup>18</sup> R. S. Nobuyasu, K. A. S. Araujo, L. A. Cury, T. Jarroson, F. Serein-Spirau, J.-P. Lère-Porte, F. B. Dias, A. P. Monkman, *J. Chem. Phys.*, 139 (2013) 164908.